

# Limits to Silicon Modulator Bandwidth and Power Consumption

Michael R. Watts, Douglas C. Trotter, Ralph W. Young,  
Anthony L. Lentine, and William A. Zortman

Sandia National Laboratory, P.O. Box 5800, Albuquerque New Mexico 87185

[mwatts@sandia.gov](mailto:mwatts@sandia.gov)

## ABSTRACT

The limits to silicon modulator bandwidth and power consumption are explored. Traditional electrical interconnects provide insufficient bandwidth ( $\sim 10\text{Gb/s}$ ) and consume far too much power ( $\sim 10\text{pJ/bit}$ ) for future high performance computing applications. Microphotonic devices closely integrated with advanced CMOS electronics have the potential to dramatically lower intra- and inter-chip communication power consumption while greatly increasing available bandwidth. Our recent results confirm the significant advantages offered by microphotonic communication links. We have broken the  $100\text{fJ/bit}$  barrier by demonstrating  $4\text{-}\mu\text{m}$  diameter microdisk modulators achieving  $10\text{Gb/s}$  data transmission with a bit-error-rate below  $10^{-12}$  and a measured power consumption of only  $85\text{fJ/bit}$ . Through rigorous simulation and experimentation, we consider ultimate limits to silicon modulator bandwidth and power consumption.

**Keywords:** Waveguide, integrated optics devices, resonators

## 1. INTRODUCTION

Communications links on high performance computers currently use electrical or directly modulated laser optical communication links that are connected to microprocessors indirectly through electrical transmission lines. In either case, the demonstrated power consumption is on the order of  $10\text{pJ/bit}$  ( $10\text{W/Tb/s}$ ), far too great for future exascale high performance computing applications with projected aggregate data rates in the exabytes/s ( $\sim 10^{19}\text{bits/s}$ ). Further, the bandwidth densities offered by multi-mode fibers do not substantially improve upon that provided by electrical transmission lines and therefore do not allow for the required multi-terabyte communications on and off microprocessor chips. However, optics, closely integrated with CMOS electronics has been proposed as a means for substantially improving upon the power consumption of electrical communications links [1]. Further, with single-mode silicon microphotronics, wavelength division multiplexing can readily be implemented [2] to drastically increase bandwidth density enabling multi-terabit-per-second communication links that are compatible with CMOS electronics.

While many silicon modulator designs have been proposed and implemented [3-5] only recently have silicon modulators broken the  $100\text{fJ/bit}$  barrier and achieved  $10\text{Gb/s}$  data rates without signal pre-emphasis [6]. This new class of silicon modulators utilizes vertical  $p\text{-}n$  junctions to maximize the overlap with the optical mode. The vertical  $p\text{-}n$  junction in a  $4\text{-}\mu\text{m}$  diameter microdisk modulator enables sufficient modal overlap to achieve  $10\text{Gb/s}$  reverse-biased operation with a low,  $3.5\text{V}$ , drive voltage and without signal pre-emphasis. A bit-error-rate (BER) below  $10^{-12}$  was demonstrated along with a measured power consumption of only  $85\text{fJ/bit}$  ( $85\text{}\mu\text{W/Gb/s}$ ), a new record for silicon modulators. Further, recent finite element simulations demonstrate the potential for  $10\text{fJ/bit}$  communications with drive voltages of only  $2.5\text{V}$ . Here, we consider limits dictated by fundamental and technological considerations on both the bandwidth and power consumption of reverse-biased  $p\text{-}n$  junction modulators. In doing so, we determine that it should be possible to achieve  $10\text{fJ/bit}$  modulator power consumption at data rates upto  $10\text{Gb/s}$ .

## 2. DESIGN

The free-carrier effect in silicon is a broadband, but relatively weak effect [7]. The broadband nature of the free-carrier effect is critical to its utility for high-bandwidth applications since the optical bandwidth of the effect determines the available bandwidth for data transmission in a modulator application. The free-carrier effect is the only semiconductor effect (aside from traditional and generally very weak nonlinearities) with an optical bandwidth that substantially exceeds one terahertz. Still, the small size of the effect, presents some innate challenges.

The change in the real and imaginary components of the refractive index as a function of carrier concentration at a wavelength of  $1.55\mu\text{m}$  is plotted in Figure 1a and 1b. The change in the real part of the refractive index is larger than that of the imaginary component. Further, the effect on the real part of the refractive index by the injection or depletion of holes is substantially larger than that produced by electrons yet the holes produce a weaker effect on the imaginary component of the refractive index. Thus, to maximize the change in amplitude, it is necessary to utilize a phase-to-amplitude converter, such as an interferometer or a resonator, and it is generally desirable to impart the change in phase with depletion of holes rather than electrons. Resonators enable small effects to be effectively multiplied up at the expense of narrowband operation. However, in wavelength division multiplexed (WDM) communication links, channels at both the transmitter and receiver need to be multiplexed and demultiplexed anyway. The multiplexing operation at the transmitter can be combined with modulation of the signal with minimal added complexity. Therefore, resonators offer substantial advantages in enhancing the rather small free-carrier effect in silicon.

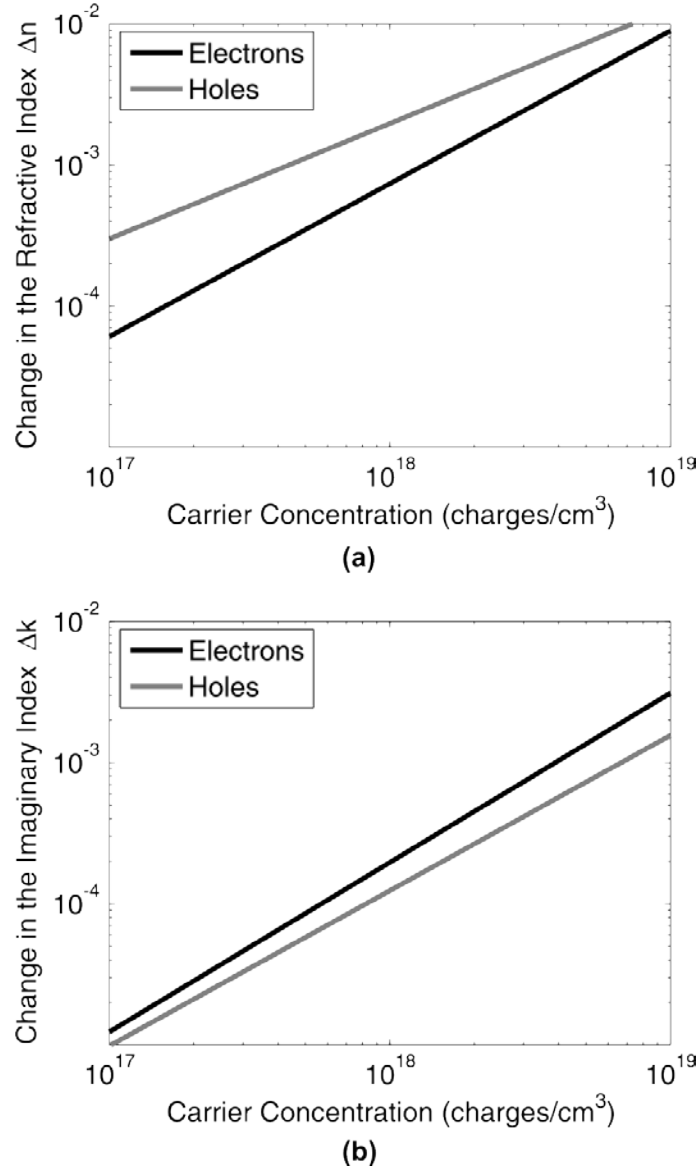


**Figure 1.** The change in the (a) real and (b) imaginary components of the refractive index compared to that of undoped silicon are plotted as a function of carrier concentration in silicon for both electrons and holes at a wavelength of  $\lambda = 1550\text{nm}$ . The change in the real part of the refractive index is larger than that of the imaginary part and impacted more greatly by holes. The plots were obtained from curve fits to the experimental data reported in [7].

Modulation via the free-carrier effect can be achieved by either injection or depletion of free-carriers. Injection offers the advantage of very large changes in the carrier concentration with low applied voltages. However, injection-based modulators are limited by the free-carrier lifetime in silicon which tends to be on the order of a few nanoseconds in small silicon waveguides [5]. As a result, injection-based modulators require signal pre-emphasis to achieve high data rates, greatly increasing power consumption and generally leading to partially closed eye diagrams. Depletion-based modulators do not suffer from free-carrier lifetime limitations, but are limited by the changes in the depletion width that are achievable. Depletion-based modulators are capacitive devices. The energy required to switch a capacitive modulator is  $CV^2$  and the energy-per-bit in a non-return-to-zero (NRZ) data transmission scheme is  $\frac{1}{4} CV^2$ . Further, the device electrical bandwidth is limited by the RC time constant. Thus, to minimize the energy-per-bit, and maximize the device bandwidth, it is desirable to have as small a modulator as possible, placing further importance on the use of resonant effects.

The realized change in the modal index is always less than the refractive index change induced at a given electron or hole concentration because the overlap with the mode of the fractional change of the depletion width is always less than unity. To maximize the overlap with the mode, the voltage should be dropped across the thinnest region of the waveguide. That is, if the waveguide is taller than it is wide, from the perspective of maximizing the size of the effect, a horizontal  $p$ - $n$  junction should be utilized. Conversely, if the waveguide is wider than it is tall, from the perspective of maximizing the size of the effect, a vertical  $p$ - $n$  junction should be utilized. Due to the difficulty of fabricating tall and

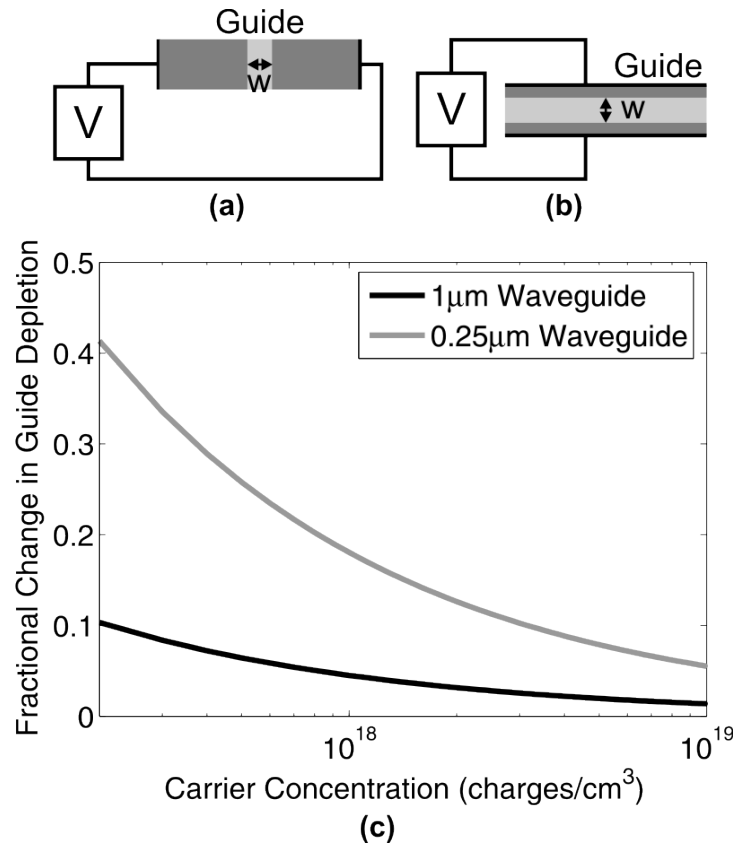


**Figure 2.** Cross-sectional diagrams of modulators formed by applying voltages across the (a) wide and (b) narrow gaps of waveguides and (c) a plot of the fractional change in the waveguide depletion obtained from the depletion approximation [8] going from 0V to 2.5V applied for a 0.25μm silicon waveguide and a 1μm waveguide. The fractional change in depletion is considerably higher for the narrow waveguide.

narrow structures, the latter case normally prevails, providing a stronger effect. And, although the gap between the contacts is smaller when the voltage is applied across the narrow dimension of the waveguide, the capacitance is dictated by the depletion width rather than the separation between the plates of the contacts. Therefore, by applying the voltage across the narrow region of the guide, a larger effect can be had with little impact on the device bandwidth. This point is

illustrated in Figure 2 where the fractional change in depletion width as a function of carrier concentration is plotted for two guide thicknesses, a narrow guide with a thickness of  $0.25\mu\text{m}$  and a thick guide with a thickness of  $1\mu\text{m}$ , for 2.5 volts applied. At a carrier concentration of  $10^{18}/\text{cm}^3$ , the narrow waveguide achieves an 18% fractional change in depletion while the wide guide achieves only a 4.5% change. Therefore, the magnitude of the effect is approximately four times larger when the voltage is applied across a narrow  $0.25\mu\text{m}$  gap versus a wide  $1\mu\text{m}$  gap, roughly corresponding to the ratios of the guide dimensions. If we consider the expected refractive index change from Figure 1a with the assumption that the electrons and holes are equally depleted, we expect a change in the effective index of  $\sim 2 \times 10^{-4}$  corresponding to a shift of  $\sim 10\text{GHz}$  in the frequency of a resonator operating a wavelength of  $1550\text{nm}$ , sufficient for a modulator operating upto  $10\text{Gb/s}$  based on realizable extinction ratios of  $10\text{GHz}$  wide resonances.

Finite-difference cylindrical mode-solver simulations indicate that microring and microdisk resonators with diameters as small as  $3.5\mu\text{m}$  can achieve radiation Q's above  $10^5$  making their radiation Q's sufficient for modulator applications. Given that the optical mode travels in only the outer  $0.75\mu\text{m}$  of a microdisk, and the depletion width at a carrier concentration of  $10^{18}/\text{cm}^3$  is  $100\text{nm}$ , it should be possible to achieve a switching energy of  $CV^2 = 12\epsilon_0\pi(r_2^2 - r_1^2)/w \cdot 2.5^2 \cong 27\text{fJ}$ , and an energy-per-bit of only  $6.75\text{fJ}$ . Technological constraints could push this number up a bit, but achieving  $10\text{fJ/bit}$  should be possible. Finite element device simulations confirm that this is in fact the case.

### 3. FABARICATION

A cross-sectional diagram and a scanning electron micrograph (SEM) of the fabricated silicon microdisk modulator are presented in Fig. 3a and 3b, respectively. The modulator consists of a  $4\mu\text{m}$  diameter microdisk resonator with a

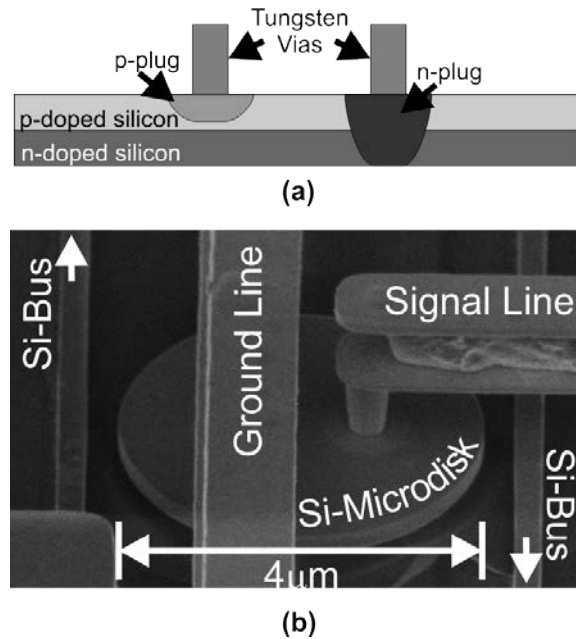


**Figure 3.** (a) Cross-sectional diagram of the microdisk modulator highlighting the vertical p-n junction and method of contact. (b) A scanning electron micrograph of the fabricated  $4\mu\text{m}$  diameter microdisk modulator.

vertically oriented *p-n* junction coupled to a pair of silicon bus waveguides. The modulator was fabricated from a silicon-on-insulator (SOI) wafer with an initial  $250\text{nm}$  silicon layer thickness and  $3\mu\text{m}$  of buried oxide. The modulator geometry was defined with an ASML Deep Ultra-Violet (DUV) laser scanner and silicon etch. Contact to the *p-n* junction was made with tungsten vias connected to highly doped p+ (B) and n+ (P) plugs. In this manner, all contacts are kept within the interior of the microdisk enabling a hard outer silicon wall of the microdisk to be maintained. This is in contrast to all previously demonstrated silicon microring modulators and it is this hard outer wall that enables maximum confinement of the whispering gallery mode and the realized  $2\mu\text{m}$  bend radius to be achieved without inducing radiation loss. Further, the use of a vertical *p-n* junction maximizes the overlap of resonator mode with the depletion width, enabling sufficient changes in the resonant frequency to be achieved with low reverse-biased voltages.

However, in this first demonstration, the  $p$ - $n$  junction was formed across the entire disk despite the fact that the resonator mode only propagates in the outer region of the disk. This simplified the mask set for fabrication but increases the switching energy and energy-per-bit of the realized modulator.

#### 4. EXPERIMENTAL RESULTS

The optical responses of the modulator with no applied bias and with a 3.5V reverse-bias voltage applied are presented in Figure 4a. With a 3.5V reverse bias, a frequency shift of -20GHz is achieved. This frequency shift is sufficient to

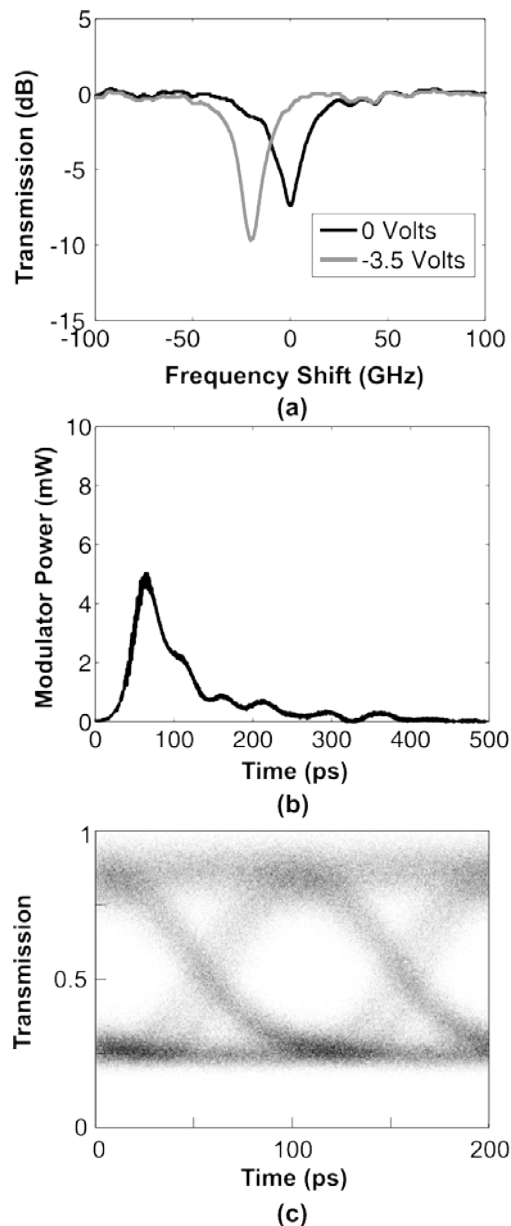


**Figure 4.** (a) The optical spectra of the microdisk in Fig. 3 with no bias and a 3.5V reverse bias applied. The center wavelength of the unbiased resonance is 1578nm. The switching energy of the modulator at a drive voltage of 3.5V was measured using electrical time domain reflectometry to be 340fJ. The modulator power consumption for a 3.5V voltage step as a function of time is plotted in (a). It is important to note that the energy/bit is one-fourth the switching energy for a non-return-to-zero (NRZ) data format since power is only consumed for 0-to-1 transitions. Therefore, the energy/bit is 85fJ. Shown in (b) is an eye-diagram for the modulator with a 10Gb/s NRZ data format with a PRBS pattern length of  $2^{31}-1$ . The bit-error-rate (BER) was measured to be less than  $10^{-12}$  for a pattern length of  $2^{15}-1$  and  $10^{-9}$  for a pattern length of  $2^{31}-1$ . The modulator was driven directly from the 1.8V output of the PRBS generator with no amplification or pre-emphasis. Due to the high impedance of the device, the voltage realized across the junction was ~3.5V.

provide 8dB of extinction between the two states. Further, this extinction ratio can readily be improved upon by removal of one of the bus waveguides and tuning in the coupling coefficients to match the losses in the modulator. However, the use of a pair of bus waveguides leaves free the option for using one of the guides as a power bus and, this extinction is sufficient for achieving good contrast in the modulated output. To determine the dynamic performance of the modulator, it was driven directly with the 1.8V output of a 10Gb/s non-return-to zero (NRZ) pseudo-random bit-stream (PRBS) generator with no signal amplification or pre-emphasis. An eye-diagram for the modulator with a 10Gb/s NRZ data format and a PRBS pattern length of  $2^{31}-1$  is presented in Figure 4c. The bit-error-rate (BER) was measured to be less than  $10^{-12}$  for a pattern length of  $2^{15}-1$  and  $10^{-9}$  for a pattern length of  $2^{31}-1$ . The increased error rate at longer pattern lengths is believed to be due to a combination of thermo-optic effects and the low received power level resulting from poor fiber-to-chip coupling.

Since one of the primary drivers in considering optical inter- and intra-chip communications networks is reducing power consumption, the required energy per transmitted bit is of equal, if not more importance, than the data rate and BER. Although the drive voltage from the PRBS was only 1.8V, the voltage realized across the  $p-n$  junction was closer to 3.5V on account of the impedance mismatch between the  $50\Omega$  line and the high impedance modulator. The power absorbed in the modulator with a voltage of 3.5V was determined by a series of small-signal time domain reflectometry measurements with step voltage inputs in  $\frac{1}{2}$ Volt increments up to 3.5V. The total power consumption was determined by comparing the difference in the power reflected when the microwave probe was in contact with the device or in contact with an open-circuited device with probe pads. The difference between these measurements is the power absorbed in the modulator and is presented in Fig. 4b. The switching energy was then determined to be 340fJ by integrating the absorbed power. This is in close agreement with the 230fJ switching energy predicted by finite element simulations. It is important to note that the 0-to-0, 0-to-1, 1-to-0, and 1-1 transitions are all equally probable in an NRZ PRBS, and since the device has essentially no dark current ( $<100\text{pA}$ ) and energy is only required to make the 0-to-1 transition, the energy/bit is  $\frac{1}{4}$  of the 0-to-1 switching energy. Therefore, the average energy/bit is 85fJ.

Traditional electrical and optical interchip communication lines require on the order of 10pJ/bit (10mW/Gb/s). Here we have demonstrated the ability to generate data at 85fJ/bit ( $85\mu\text{W/Gb/s}$ ) or approximately two-orders of magnitude less than more traditional techniques. Moreover, since the switching energy is simply  $CV^2$ , more intricate doping profiles that are limited primarily to the outer regions of the disk where the optical mode resides will reduce the capacitance and the required energy/bit below 10fJ. And while the power consumption of the laser source and the receiver have not been taken into account, it can be argued that the power consumption of these components will be less than 10fJ/bit. The arguments are based on the idea that with low capacitance receivers, CMOS logic gates can be driven directly without the need for amplification [1].

As a final point, high-speed, high-order bandpass switches can be constructed from multiple modulators coupled together. An SEM of a fabricated and previously demonstrated [6] structure is shown in Fig. 5a and the filter response depicted in Fig. 5b as a function of applied forward bias along with the dynamic response of the switch demonstrating greater than 16dB extinction in the Thru port and 20 dB extinction in the Drop port with a  $\sim 2.4\text{ns}$  switching time (Fig. 5c). Such high-speed silicon bandpass switches can be used to route data in the optical domain in future high-performance computers.

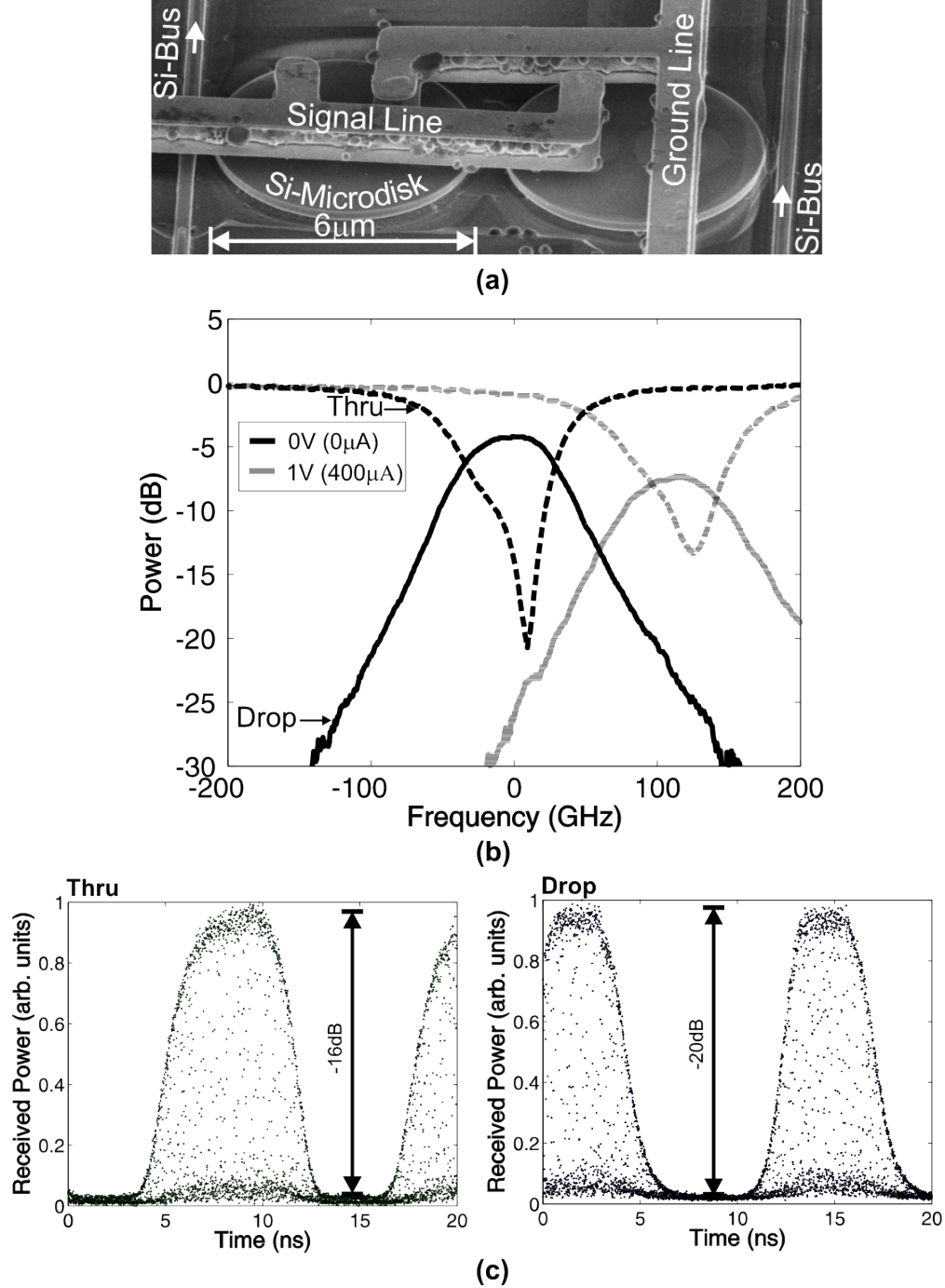


**Figure 5.** (a) Cross-sectional diagram of the microdisk bandpass switch. (b) The bandpass of the switch under 0V and 1V applied bias and (c) the dynamic response of the switch in the Thru and Drop ports switching 10Gb/s data. The center wavelength is 1533nm.

#### 4. CONCLUSIONS

We have explored critical design elements affecting the performance of silicon modulators. Back of the envelope calculations, supported by finite element simulations, indicate that achieving an energy-per-bit below 10fJ should be possible in a resonant silicon modulator. In an experimental demonstration, utilizing a *p-n* junction, oriented across the narrow, vertical dimension of silicon microdisk resonator, we were able to demonstrate the lowest drive voltage, highest-

speed, and smallest silicon resonant modulator demonstrated to date. As a result of the low drive voltage and small device size, we were able to demonstrate the first silicon microphotonic modulator to achieve less than 100fJ/bit in digital communications despite a rather simple and inefficient doping profile. Further, this modulator represents the first resonant silicon modulator to achieve 10Gb/s data transmission without signal pre-emphasis. As a final note to this work, high speed silicon bandpass switches were constructed by coupling a pair of modulators together to form an active second-order filter. These second order filters were switched by injecting carriers into the  $p$ - $n$  junction at a 2ns switching speed achieving -16dB extinction in the Thru and -20dB extinction in the Drop port, representing the first high-speed silicon bandpass switches demonstrated to date. Together with high-speed, low-power, bandpass switches, microdisk modulators have the potential to form the building blocks for richly interconnected short-range optical networks such as the three-dimensional mesh networks connecting high-performance supercomputers.

## 5. ACKNOWLEDGMENTS

Sandia is a multiprogram laboratory operated by Sandia Corporation, a Lockheed Martin Company, for the United States Department of Energy's National Nuclear Security Administration under contract DE-AC04-94AL85000. Partial funding for this work was provided by the DARPA Microsystems Technology Office.

## 6. REFERENCES

1. D. A. B. Miller, "Optics for low-energy communication inside digital processors, quantum detectors, sources, modulators as efficient impedance converters," *Optics Letters*, **14**, 1460-148 (1989)
2. T. Barwicz, M. R. Watts, M. A. Popovic, P. T. Rakich, L. Socci, F. X. Kärtner, E. P. Ippen and H. I. Smith, "Polarization-transparent microphotonic devices in the strong confinement limit," *Nature Photonics* **1**, 57 – 60 (2006)
3. William M. Green, Michael J. Rooks, Lidija Sekaric, and Yurii A. Vlasov, "Ultracompact, low RF power, 10 Gb/s silicon Mach-Zehnder modulator," *Optics Express*, **15**, p. 17106 (2007)
4. A. Liu, R. Jones, L. Liao, D. Samara-Rubio, D. Rubin, O. Cohen, R. Nicolaescu, and M. Paniccia, "A high-speed silicon optical modulator based on a metal-oxide-semiconductor capacitor," *Nature* **427**, 615-618 (2004)
5. Q. Xu, B. Schmidt, S. Pradhan and M. Lipson, "Micrometre-scale silicon electro-optic modulator," *Nature* **435**, 325-327 (2005)
6. M. R. Watts, D. C. Trotter, R. W. Young, and Anthony L. Lentine, "Ultralow Power Silicon Microdisk Modulators and Switches," *IEEE Group IV Photonics*, Sorrento (2008)
7. R. A. Soref, and B. R. Bennett, "Electrooptical Effects in Silicon," *IEEE J. Quantum Electronics*, QE-23, pp. 123-129 (1987)
8. Neamen, D. A., "Semiconductor Physics and Devices ", McGraw Hill Higher Education, New York, 3rd Edition (2002)
9. M. R. Watts, D. C. Trotter, and R. W. Young, "Maximally Confined High-Speed Second-Order Silicon Microdisk Switches," *OFC 2008 PDP14*